Science of the Total Environment 806 (2022) 151202

Contents lists available at ScienceDirect

Science of the Total Environment

journal homepage: www.elsevier.com/locate/scitotenv

Effects of hygroscopic growth of ambient urban aerosol particles on their modelled regional and local deposition in healthy and COPD-compromised human respiratory system

Árpád Farkas [a,*], Péter Füri [a], Wanda Thén [b], Imre Salma [c,*]

[a] Center for Energy Research, Konkoly-Thege M. út 29–33., H-1121 Budapest, Hungary
[b] Hevesy György Ph.D. School of Chemistry, Eötvös Loránd University, P.O. Box 32, H-1518 Budapest, Hungary
[c] Institute of Chemistry, Eötvös Loránd University, P.O. Box 32, H-1518 Budapest, Hungary

HIGHLIGHTS

- Depositions of ultrafine particles sensitively change due to hygroscopic growth.
- Hygroscopicity of sub-micrometer particles was experimentally determined.
- Lung deposition of ultrafine particles for healthy and COPD subjects were modelled.
- Ultrafine depositions in healthy subjects decreased in contrast to larger particles.
- For COPD patients, the hygroscopicity affected the depositions very differently.

GRAPHICAL ABSTRACT

ARTICLE INFO

Article history:
Received 18 July 2021
Received in revised form 14 October 2021
Accepted 20 October 2021
Available online 28 October 2021

Editor: Philip K. Hopke

Keywords:
Lung model
COPD
Particle deposition
Ultrafine aerosol
Hygroscopicity

ABSTRACT

Total, regional and local deposition fractions of urban-type aerosol particles with diameters of 50, 75, 110 and 145 nm were modelled and studied in their dry state and after their hygroscopic growth using a Stochastic Lung Model and a Computational Fluid and Particle Dynamics method. Healthy subjects and patients with severe chronic obstructive pulmonary disease (COPD) were considered. The hygroscopic growth factors (HGFs) adopted were determined experimentally and represent a real urban-type environment. The hygroscopic growth of particles resulted in decrease of the deposition fractions in all major parts of the healthy respiratory system and the extent of the deposited fractions was rising monotonically with particle size. In the extrathoracic (ET) region, the relative decrease was between 7% and 13%. In the lungs the deposition decreased by 11–16%. The decrease of deposition fraction due to hygroscopic growth was more accentuated in the conductive airways (up to 25%) and less pronounced towards the terminal airways. The spatial distribution of the deposited particles remained highly inhomogeneous with some areas containing thousands times more particles than the average number of particles per unit surface area. For COPD patients, the hygroscopic growth produced similar deposition alterations in the ET region than for healthy subjects. In the conductive airways, however, the particle growth caused a substantial relative decrease in the deposition fractions. In contrast, the relative depositions of hygroscopic particles increased in the acinar region.

© 2021 The Authors. Published by Elsevier B.V. This is an open access article under the CC BY license (http://creativecommons.org/licenses/by/4.0/).

* Corresponding authors.
E-mail addresses: farkas.arpad@ek-cer.hu (Á. Farkas), salma.imre@ttk.elte.hu (I. Salma).

https://doi.org/10.1016/j.scitotenv.2021.151202
0048-9697/© 2021 The Authors. Published by Elsevier B.V. This is an open access article under the CC BY license (http://creativecommons.org/licenses/by/4.0/).

1. Introduction

Poor air quality associated with high concentrations of particulate matter (PM) is one of the greatest health concerns for humans worldwide (Lelieveld et al., 2015; Cohen et al., 2017). Acute and chronic adverse health effects of aerosol particles have been documented in both toxicological and epidemiological studies in terms of increased morbidity and mortality (e.g. Valavanidis et al., 2008; Heal et al., 2012; Apte et al., 2015; Riediker et al., 2019 and references therein). Due to the chemical and physical complexity in composition, size and shape of particles and additional possible synergism with other pollutants, multiple factors are involved in the pathogenesis of diseases resulting from exposure to PM. Therefore, it cannot be expected that a single or a few aerosol dose metrics for risk assessment fully or even broadly express the induced biological responses. From the group of the relevant factors, the size of particles is an outstanding property since it is related directly to the particle deposition in the respiratory system and indirectly to the chemical composition and many other aerosol properties (Salma et al., 2002).

Particle size is primarily determined by source processes. It can further change in the air in many ways in space and time. Particle diameter growth or shrinkage by exchanging water vapour with the surrounding air as relative humidity (RH) changes is one of the most important possibilities. This can also happen inside the human respiratory system as a special compartment since the ordinary ambient RHs in most locations in the world are below the RH in the lung. Water vapour most sensitively influences the size of ultrafine (UF) particles (with an equivalent diameter <100 nm). Their role in exposure studies has been increasingly recognised (Löndahl et al., 2014; Jakobsson et al., 2018; Riediker et al., 2019) due to their excess health risk relative to coarse or fine particles of similar chemical composition (Oberdörster et al., 2005; Kreyling et al., 2002, 2006; Morawska et al., 2008; HEI Review Panel, 2013). This was associated with their relatively large number concentrations (daily medians up to 10^5 cm^{-3}), high abundances (70–90% of all particles), large total surface area and very small size of these particles (Carvalho et al., 2011; Braakhuis et al., 2014). Such conditions occur in large cities (Harrison and Jones, 2005).

Airway deposition of the inhaled UF particles depends sensitively on their diameter (thus also on RH) since their deposition is primarily governed by Brownian diffusion. As diffusivity is size-specific, it is expected that the size change due to hygroscopic growth in the airways affects the amount and spatial distribution of the deposited particles.

The hygroscopicity of particles is quantified by hygroscopic growth factor (HGF). This is the ratio of the particle diameter measured at an elevated RH to the dry particle diameter (at RH < 10%; Swietlicki et al., 2008). The HGFs depend upon RH and chemical and physical properties of particles. Ambient particles have been classified into the groups of 1) nearly-hydrophobic particles (HGF = 1.0–1.11 for 100 nm particles at RH = 90%), 2) less-hygroscopic particles (HGF = 1.11–1.33), 3) more-hygroscopic particles (HGF = 1.33–1.85) and 4) seasalt particles (HGF > 1.85; Liu et al., 2011; Vu et al., 2021). Some specific aerosol types, e.g. various smoke particles mainly from wood and vegetable oils with and without flame in general can have even higher HGFs (Dua and Hopke, 1996).

To investigate and reveal the influence of hygroscopic properties on the particle deposition in the human respiratory system, realistic urban HGFs under subsaturated conditions close to those in the respiratory system are required from the aerosol point of view. The differences in the deposition of dry and wet particles can be calculated. All this requires special experimental data and advanced mathematical modelling, which have been covered only in limited number of studies (Löndahl et al., 2007). Vu et al. (2015) have analysed regional airway deposition of hygroscopic submicrometer particles originating from different sources (atmospheric nucleation, traffic, biomass burning) and places (seaside, urban and countryside environment). They have found that the deposition efficiency of particles with dry diameters <200 nm in healthy adults was lower than for non-hygroscopic particles of the same dry size. The analysis was later extended to indoor aerosol particles with dry diameters of 50, 100 and 200 nm originating from different activities (Vu et al., 2017). The authors also determined the hygroscopic growth factors and quantified the amounts of particles deposited in different anatomical airway regions.

Experimental data or modelled results for vulnerable groups such as individuals with respiratory diseases are even more limited and are usually constrained to non-hygroscopic UF particles (Aaltonen et al., 2018; Jakobsson et al., 2018 and references therein). Rajaraman et al. (2020) studied airway deposition of (hygroscopic) NaCl particles in severe asthmatics, but only supermicrometer (1–8 μm) particles were considered. This work revealed that the increase of the deposition fractions due to hygroscopic growth was higher in asthmatics than in their healthy counterparts. Systematic studies on the effect of hygroscopic growth of UF particles in healthy and diseased airways have been still missing. Similarly, the effect of hygroscopicity on the degree of the local deposition inhomogeneity within the airways is another unexplored research field.

The pre-requisites for conducting such research for the urban Budapest are met as the specific experimental data are accessible (Enroth et al., 2018) and a considerable long-term experience and expertise with various human particle deposition models are also available (Salma et al., 2015; Farkas et al., 2019, 2020). The general aim of this research is to study the effects of hygroscopic diameter growth of UF urban aerosol particles on their regional and local depositions within the airways of both healthy and diseased subjects. Chronic obstructive pulmonary disease (COPD) was considered for this purpose. Our specific objectives are 1) to determine and interpret the relative changes in regional deposition fraction of particles with dry diameters of 50, 75, 110 and 145 nm due to hygroscopic growth in the human respiratory system, 2) to derive the local deposition pattern in a bifurcation unit in order to quantify the site-specific particle deposition and 3) to compare the results and conclusions obtained for healthy subjects and patients suffering from COPD. The combination of realistic urban-type aerosol, experimentally determined hygroscopicity growth factors, diameter growth specifically for UF size fraction (for which this effect is substantial), and healthy and COPD-compromised human respiratory systems represents an important novelty. Furthermore, we derived most results for separate airway generations and even locally, within a bifurcation unit. We also adopted two complementary approaches, namely the analytical deposition modelling and Computational Fluid and Particle Dynamics (CFPD) modelling and interpreted some of their outcomes jointly.

2. Methods

The behaviour of inhaled hygroscopic particles in the human respiratory system was studied by two different models. The deposition of particles in the whole respiratory tract and in its major anatomical regions was quantified by a Stochastic Lung Model, while the local features of the deposition were investigated by a CFPD method. Hygroscopic properties were derived experimentally for real urban aerosol by a Volatility-Hygroscopicity Tandem Differential Mobility Analyzer (VH-TDMA) measurement system.

2.1. Experimental part

The experimental work was performed at the Budapest platform for Aerosol Research and Training (BpART) Laboratory (N 47° 28′ 30″, E 19° 3′ 45″, 115 m above mean sea level; Salma et al., 2016). The location represents an average atmospheric environment for central Budapest.

The VH-TDMA system was deployed from 9 December 2014 to 9 February 2015 (Enroth et al., 2018). Its sampling inlet was set up at a height of 12 m above the street level. The humidifier track quantified the changes in electrical mobility diameter from the dry state

(RH < 10%) of particles to their humidified state. The latter was realised at a mean RH and standard deviation (SD) of (90.0 ± 0.4)%. This is commonly regarded as the standard humidification level. Atmospheric quasi-monodisperse particles with median dry diameters of 50, 75, 110 and 145 nm having GSDs of <1.25 were selected for the measurements. The instrument was operated according to international recommendations (Gysel et al., 2009; Massling et al., 2011).

The distributions of the HGF exhibited bimodal feature. The mean HGF and SD of the mode with the smaller HGF values was 1.07 ± 0.02, and it contained (69 ± 17), (53 ± 16), (47 ± 13) and (41 ± 11)% of all particles for the diameters of 50, 75, 110 and 145 nm, respectively. The corresponding mean growth factor and its SD for the mode with the larger HGF values was 1.35 ± 0.03. The contributions of this mode to the particle numbers were (31 ± 17), (47 ± 16), (53 ± 13) and (59 ± 11)%, respectively for the same set of particle diameters. The mode with the smaller HGF values represents nearly-hydrophobic (NH) particles (e.g. with high abundance of soot), whereas the other mode is associated with less-hygroscopic (LH) particles (containing e.g. organic compounds; Salma et al., 2020, 2021).

2.2. Deposition calculations

2.2.1. Stochastic lung model

The model of the whole respiratory tract applied in the present study was originally developed by Koblinger and Hofmann (Koblinger and Hofmann, 1990; Hofmann and Koblinger, 1990). Many extensions and improvements were adopted to it since then (e.g. Balásházy et al., 2007, 2009; Winkler-Heil et al., 2014; Sturm, 2016). Its advantages and status among the other particle deposition models were discussed by Asgharian et al. (2009) and Hofmann (2011). In the model, the human airways are divided into extrathoracic (ET), tracheobronchial and acinar parts. Particles can deposit in this geometry by inertial impaction, sedimentation (gravitational settling) and Brownian diffusion mechanisms. The inhaled particles are tracked through the airways until they are deposited or exhaled. The deposition in the ET airways is computed using empirical formulas (Hofmann and Koblinger, 1992). In the tracheobronchial airways, the path of particles is simulated in an asymmetric bifurcating tubular structure. Airway lengths, diameters, branching angles and gravity angles are selected by Monte Carlo method from the distributions of these morphometric parameters described by Raabe et al. (1976). The geometry of the acinar airways is reconstructed on the basis of the description by Haefeli-Bleuer and Weibel (1988). The model provides the fractions of the inhaled particles which are deposited in the three major parts of the respiratory system and also in each airway generation.

The deposition by Brownian diffusion becomes the dominant mechanism for particle sizes below approximately 100 nm. This process is represented by mobility diameters. Impaction and sedimentation – which are related to aerodynamic diameter of particles – become the controlling mechanisms above 1 μm (Salma et al., 2015). The effects of diffusion and impaction become very similar to each other at 400–500 nm, depending on the physical activity of the subjects. This all means that the size distributions expressed in the mobility diameter representation capture the real deposition behaviour of the particles correctly in the diameter interval considered here.

Quiet nasal breathing of healthy male adults was considered for the study. This resembles sitting physical activity. The higher reference physical activities are not very relevant for diseased subjects (see Sect. 2.2.2), and this would also make the comparison of the healthy and diseased lungs questionable. The following breathing parameters were adopted: functional residual capacity (FRC) of 3300 cm^3, tidal volume (VT) of 750 cm^3 and breathing cycle time (t) of 5 s. The inhalation and exhalation times were set to be identical (ICRP (International Commission on Radiological Protection), 1994). The computations were carried out considering both particles with dry and dynamically changing wet diameters. The efficiency of particle deposition was expressed in terms of deposition fractions defined as the ratio of the number of particles deposited in an airway segment to the number of inhaled particles. The change due to the hygroscopic growth was quantified as the difference between the wet and dry deposition fractions over the dry deposition fraction.

2.2.2. COPD model

The Stochastic Lung Model with modified airway geometry module was applied to simulate the particle transport and deposition within the diseased airways. Severe COPD symptoms were considered with seriously affected lung structure and breathing capacity. Regarding the airway geometry, it was assumed that the airway ducts are constricted, whereas the alveolar airspaces are enlarged. Unfortunately, these changes could not be measured by computer tomography because its spatial resolution was not sufficient for investigating the small airways. Instead, the contraction parameters used in the calculations were estimated from complex spirometric data and pulmonary function tests of diseased subjects (Horváth et al., 2009; Füri et al., 2017). In the bronchial airways, the probability of the contraction was considered to be 100%, and its minimum and maximum extents were 0% and 40%, respectively for all (1−21) airway generations. In the acinar region, the contraction probability was considered to be 100%, while its minimum and maximum were 30% and 100%, respectively (over the 12 acinar generations). The actual extent of the contraction was randomly selected from these ranges for each bifurcation unit during the airway deposition distribution simulations. The data adopted are in accordance with the general pathological description of the disease. For the emphysema, the probability of contraction of the duct was set to 100% and the extent of the contraction of the ducts varied from 30% up to 100%. The probability of the alveolus enlargement was set to 90% and its extent was expressed by a factor from 200% to 5000%. These conditions correspond to the concomitant presence of bronchitis and bullous type emphysema. We have to add that, due to the stochastic nature of the lung model, the deposition distributions are the mean values of the deposition probabilities for 10,000 particle pathways, which is expressed by the mean tubular diameter. In addition, the number of the bronchial and acinar generations can also vary among the runs. This means that the airway generations from 12 to 21 can belong to bronchial or acinar regions, which is handled in the model. To indicate the difference between the diameters for a healthy subjects and a severe COPD patients, the mean airway diameters obtained are specified in Table 1.

The deposition in the diseased lung is influenced not only by the change in the airway geometry, but the lung compliance also contributes (Choi et al., 2019). The modified compliance was taken into account indirectly and uniformly through COPD-specific breathing parameters (lung volumes and capacities, and breathing profile) in the following manner. 1) The reduced elasticity of lung parenchyma leads to modified compliance, namely to the shifting of the relationship between the lung volume and distending pressure in a way that a given lung volume in COPD patients produces smaller recoil pressure than in the healthy lung (Fergusson, 2006). Combined with expiratory flow limitations, this leads to hyperinflated lung (Papandrinopoulou et al., 2012) with increased residual volume, which implies increased FRC. We modelled the tidal breathing in a manner that the starting volume was set to the FRC. Its value was increased to 4500 cm^3 in COPD patients (from 3300 cm^3 in healthy subjects, Sect. 2.2.1). Mathematically, this was achieved by rescaling the initial lung to have larger volume at the end of the expiration. 2) To accommodate the increased respiratory demands, the minute ventilation (flow rate) increases in COPD patients, which leads to higher breathing frequency. We also took this effect into account by reducing the breathing cycle time of $t = 5$ s (for healthy lung, Sect. 2.2.1) to 2 s. 3) The inhalation time to exhalation time ratio also decreases due to the disease. This was also taken into account by decreasing the ratio from 1 (healthy subject) to 0.5 (COPD patient). 4) There is evidence that the minute volume in COPD patients increases mostly due to the decrease of the breathing time. This limitation is

Table 1
Mean diameter of the airway (in cm) tubes in healthy and COPD-compromised human respiratory system of an adult male performing sitting physical activity.

Airway generation	Healthy subject	COPD patients
1	1.75	1.53
2	1.35	1.18
3	1.08	0.94
4	0.92	0.80
5	0.77	0.67
6	0.67	0.58
7	0.56	0.49
8	0.49	0.43
9	0.40	0.34
10	0.32	0.28
11	0.24	0.21
12	0.189	0.164
13	0.149	0.127
14	0.119	0.097
15	0.096	0.073
16	0.078	0.055
17	0.066	0.041
18	0.058	0.031
19	0.051	0.024
20	0.046	0.020
21	0.041	0.016

consistent mainly at higher physical activities. There are, however, also data which indicate slightly lower tidal volumes at rest as well (O'Donnell et al., 2001). Therefore, we lowered the VT slightly from 750 to 600 cm^3. The set of the corresponding parameters was determined from our previous spirometric measurements on diseased subjects. The input data utilised represent a sensible approximation to reality and reflect the changes in airway compliance due to COPD.

Beyond the modified airway geometry, the COPD specific breathing parameters (particularly the modified flow rate) substantially influence the airflows and the subsequent particle deposition. This was adopted by modifying the air and particle velocities and residence times in the deposition formulas in addition to the altered airway caliber. These details were dealt with in our previous modell-oriented publications (Horváth et al., 2009; Füri et al., 2017).

The remaining limitation regards the possibly asymmetric character of the damage due to the COPD. This can eventually lead to local inhomogeneities in the compliance and to modified ventilation. In this sense, the results obtained by the present COPD model are still subject to larger uncertainty and further improvements are feasible.

2.2.3. Computational fluid and particle dynamics model

Previous studies demonstrated that the local deposition of particles is highly nonuniform with local deposition maxima at the peak (carina) of individual airway bifurcations (e.g. Farkas and Balásházy, 2008). We studied the possible effects of the hygroscopic growth on the inhomogeneous deposition pattern by a CFPD method. An airway bifurcation from the right upper lobe corresponding to the airway generations of 4–5 (if trachea is labelled as 1) was selected to represent the bronchi in the large bronchial airways. Symmetric branching and air flows were only considered (Fig. 4a). The three-dimensional digital airway was spatially discretized by the construction of a computational mesh. The mesh contained tetrahedral core cells and prismatic boundary layers. A mesh independence test was performed by comparing the air velocity profiles at different locations for meshes with different cell sizes resulting in an appropriate mesh size of 4.8×10^6 numerical cells. Steady inspiratory airflow was modelled by k-ω SST turbulence model with low-Reynolds number correction, where k is the turbulent kinetic energy and ω is the specific turbulent dissipation rate. Parabolic velocity profile corresponding to 30 L min^{-1} tracheal volumetric flow rate (3.75 L min^{-1} at entrance of the target bifurcation) was assumed at the parent branch inlet, and pressure outlets with zero-gauge pressure were prescribed as boundary conditions. The deep lung compliance is one of the main drivers of the air flow at the regional level. Our previous comparative investigations showed, however, that the non-identical pressure values at the outlets of daughter tubes do not seem to influence substantially the effect of the hygroscopic growth and the trends in the deposition inhomogeneity for a single airway bifurcation. This conclusion appears to be related to the combination of the deposition mechanisms, which change slowly with air flow characteristics in the considered range. Individual particles were tracked in the computed airflow field treated as a continuum (Euler–Lagrange approach). One way coupling between the discrete and continuous phases was assumed, namely that the particles were influenced by the airstreams, whereas the air flow was independent of the movement of the particles.

The transport equations of mass, momentum, turbulent kinetic energy and turbulent specific dissipation rate were solved numerically by the solver of the commercially available ANSYS FLUENT software. A finite volume method was applied to numerically solve the mathematical equations describing the air flow. The particle force balance equation was written and solved for every individual particle. If a particle trajectory intersected the airway wall then the particle was considered to be deposited and the related coordinates were recorder.

The deposition in the studied single airway bifurcation was quantified in terms of the deposition efficiency. This is the ratio of the number of particles deposited in the bifurcation to the number of particles that enter the bifurcation. The degree of inhomogeneity of the particle deposition within the bifurcation was quantified by the enhancement factor. This is the ratio of the deposition density on a small surface to the deposition density for the whole bifurcation area. The deposition density is the ratio of the number of particles deposited on a surface element to the area of that surface element. The enhancement factors were calculated by scanning along the whole surface with a pre-specified surface element (patch) and counting the number of deposited particles on that patch. The enhancement factors depend on the surface area of the patch. A patch size of 3 mm^2 was selected, which corresponds to an area of an epithelial cell cluster containing approximately 10,000 biological cells (Devalia et al., 1990).

2.3. Hygroscopic growth

The distribution of RH along the human airways was documented in pioneering studies. At the tracheal inlet, the air humidity was described by Perwitzschky (1928). Ingelstedt (1956) reported the RH values at the level of larynx. Later, Keck et al. (2000) published the RH values in the upper airways as a function of the distance from the nostril. These data are summarized in Fig. 1, which also shows the evolution of the RH in the naso-pharyngeal-laryngeal-tracheal route. The locations of the pharynx, laryngeal cavity and tracheal inlet are also indicated on the basis of the anatomical data of Bates et al. (2015). A RH of 60% was assumed for the ambient air, which is typical for the study site (Mikkonen et al., 2020) and acceptable for many other continental environments in middle latitudes. Fig. 1 also shows that the particle sizes as measured at a RH = 90% can be utilised in the computations only for the upper airways, where the mean RH is around 92%.

This is, however, a plausible approximation if the time needed for particles to grow from the ambient conditions to their size at a RH = 90% is comparable to their residence time in the upper airways. Such calculations performed by the Stochastic Lung Model revealed that during quiet nasal breathing, particles spend approximately 1.2 s in the upper airways from their inhalation until their entrance into the trachea. At the same time, Ferron (1977) demonstrated that particles smaller than 200 nm reach their final size in ca. 0.1 s at the relevant RHs in the lung, except for those which contain surfactants or start as crystalline or amorphous glassy particles. The particles dealt with in the present research can be reasonably assumed to respond fast or instantaneously to the moisture content and reach their equilibrium size in the upper airways during inhalation. The particle diameters

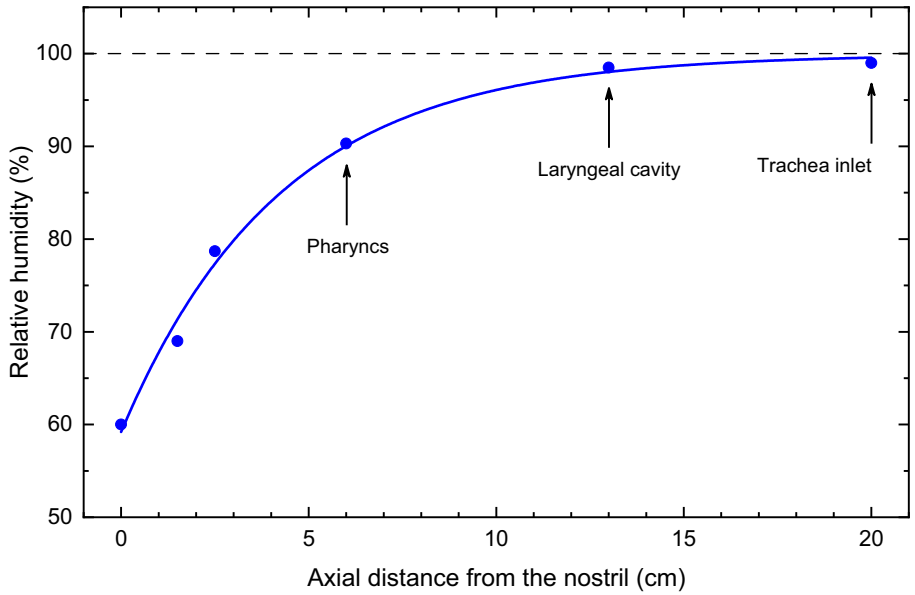

Fig. 1. The dependency of the relative humidity in the upper airways of the human respiratory system on the distance from nostril towards the lung. The line was obtained by fitting with an exponential increase function and serves to guide the eye.

measured at a RH = 90% represent their actual size at the entrance to the lung.

In the lung, the RH becomes between 98% and 99.9% (Perwitzschky, 1928). In line with previous investigations (e.g. Vu et al., 2015), a RH = 99.5% was applied for the lung for both inhalation and exhalation. The same value was adopted in the upper airways at exhalation. The particle diameters at RH were estimated by using the Rissler approximation (Rissler et al., 2006; Kristensson et al., 2013):

$$\mathrm{HGF}(99.5\%) = \left(1 + \left(\mathrm{HGF}^3(a\%) - 1\right) \times \frac{99.5\%}{a\%} \times \frac{100 \times \exp\left(D_p \times \mathrm{HGF}(99.5\%)\right) - 99.5\%}{100 \times \exp\left(D_p \times \mathrm{HGF}(a\%)\right) - a\%}\right)^{\frac{1}{3}}, \quad (1)$$

where HGF(99.5%) is the hygroscopic growth factor at a RH of 99.5%, HGF(a%) denotes the hygroscopic growth factor at an arbitrary a% RH and D_p is the dry particle diameter. The formula is a simplified equation of a more general expression derived from the classical Köhler theory. In this study, the parameter a% was equal to 90%. As Eq. (1) contains the needed HGF(99.5%) implicitly, a numerical root finder algorithm was applied to determine its value.

3. Results and discussion

3.1. External mixture of particles

Ambient aerosol particles in cities including Budapest often form external mixtures with distinct hygroscopic properties (Enroth et al., 2018; Salma et al., 2021). The HGFs for nearly-hydrophobic and less-hygroscopic particles determined experimentally at a RH = 90% were adopted directly in modelling the upper airways, whereas they were scaled to RH = 99.5% to represent the lung. The results are summarized in Table 2. In the lung, the particle diameters increased by approximately 15% for NH particles and by ca. 60% for LH particles. In addition to this growth, the two types of particles were considered in the calculations also by selecting the inhaled particles in accordance with the number fractions of these two externally mixed modes (see Sect. 2.1). These abundances represent realistic urban conditions.

3.2. Regional deposition in healthy subjects

The deposition fractions of non-hygroscopic polydisperse UF urban particles in the tracheobronchial region of the respiratory system obtained by similar modelling than in the present work were nearly constant (9–14%) for different physical activities, while the deposition fractions in the acinar region increased monotonically with physical activity from approximately 14% for sleeping to 35% for heavy exercise (Salma et al., 2015). Consequently, the deposited fractions in the lung increased with the level of the physical activity from 25% (sleeping) to 49% (heavy exercise). At the same time, the deposition fraction of particles in the ET region decreased monotonically from approximately 30% to 8% with physical activity. The present results calculated for selected monodisperse dry diameters inhaled during quiet breathing were in line with the above values.

More importantly, as shown in Fig. 2, the deposition fractions systematically decreased in all major regions of the respiratory system due to the hygroscopic growth. (Note that the figure displays the decrease, so positive values actually represent deposition decrease.) This can be explained by the main deposition mechanism. The deposition by thermal diffusion prevails over the impaction and sedimentation in the studied diameter range. The effect of the diffusion became extensively smaller with particle size, while the impaction and sedimentation increased only slightly. In the ET region, the relative decrease of the deposition fraction was between 7% and 13%. As the particles reached their maximum diameter in the lung, the relative decrease (of 11–16%) was the highest in this region. In addition, its extent rose monotonically

Table 2
Hygroscopic growth factors for nearly-hydrophobic particles and less-hygroscopic particles derived experimentally for different dry particle diameters (D_d in nm) at a RH of 90% (representing the upper airways) and recalculated for RH = 99.5% (representing the lung).

D_d/RH	50	75	110	145
Nearly-hydrophobic particles				
90%	1.07	1.07	1.09	1.09
99.5%	1.14	1.14	1.18	1.18
Less-hygroscopic particles				
90%	1.31	1.35	1.37	1.37
99.5%	1.55	1.61	1.65	1.65

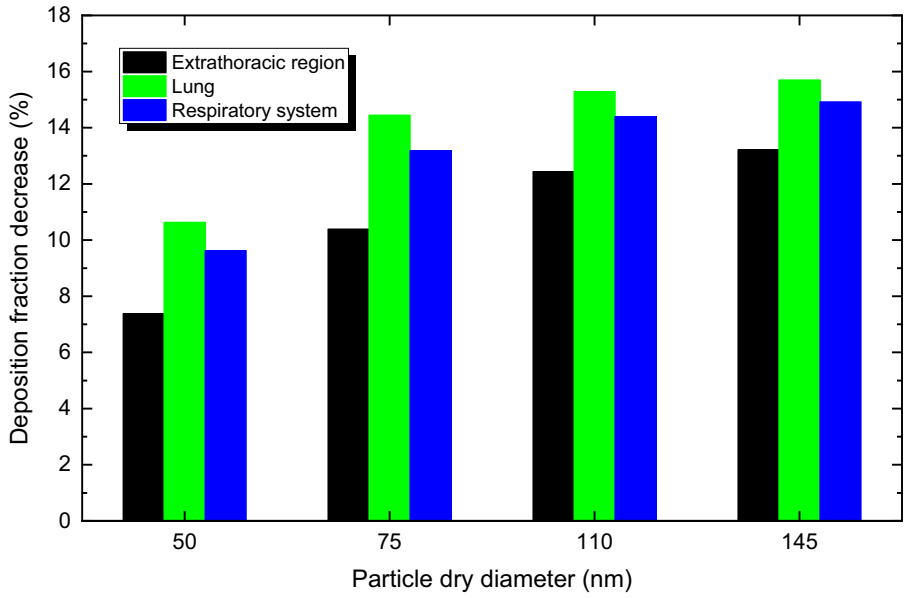

Fig. 2. Relative decrease of regional deposition fractions due to hygroscopic growth of urban aerosol particles with different dry diameters in the extrathoracic region, lung and the whole human respiratory system.

with particle size. This was mainly caused by the larger HGFs and higher abundances of LH particles with respect to NH particles for larger sizes (Table 2 and Sect. 2.1).

The relative decrease of the deposition fraction due to the hygroscopic growth as a function of airway generation number is shown in Fig. 3. It can be seen that the decrease occurred in all airway generations, but it was not completely homogeneous along them. There was a tendency for lower relative decrease with increasing airway generation number. This was perhaps more evident at the larger generation numbers although it was disturbed by inter-airway fluctuations. The highest relative decrease (up to ca. 25%) was found in the large bronchial airways.

The pattern seen in Fig. 3 resulted from different deposition mechanisms for different particle sizes in the various parts of the airways. The hygroscopic growth caused an increase of the deposition by impaction and sedimentation, but also a deposition decrease by Brownian diffusion. As the diffusion is the dominating deposition mechanism in the studied size range, the overall effect yielded in a decrease. In addition, the dominance of the diffusion was lower in the smaller airways (generations 15–20), which lead to lower deposition decrease. The inter-generational fluctuations in the relative decrease are likely a result of the change of airway structure to a higher extent and of the changes of the airway dimensions to a smaller extent. The gradual transition from bronchial ducts to alveolated airways (at generation numbers of 15–17) caused the highest fluctuations, while a relative stabilization tendency could be observed in the fully alveolated airways. It is worth noting that the higher dry diameters were generally associated with higher extents of relative deposition decrease, whereas local fluctuations considerably perturbed the monotonical behaviour.

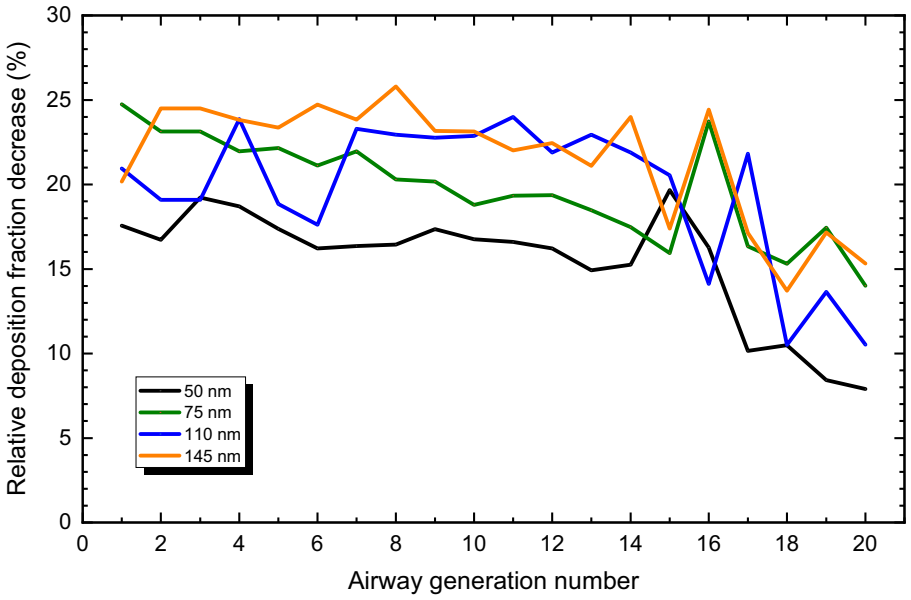

Fig. 3. Relative decrease of particle number deposition fractions in the airway generations of healthy subjects due to hygroscopic growth for urban particles with different dry diameters.

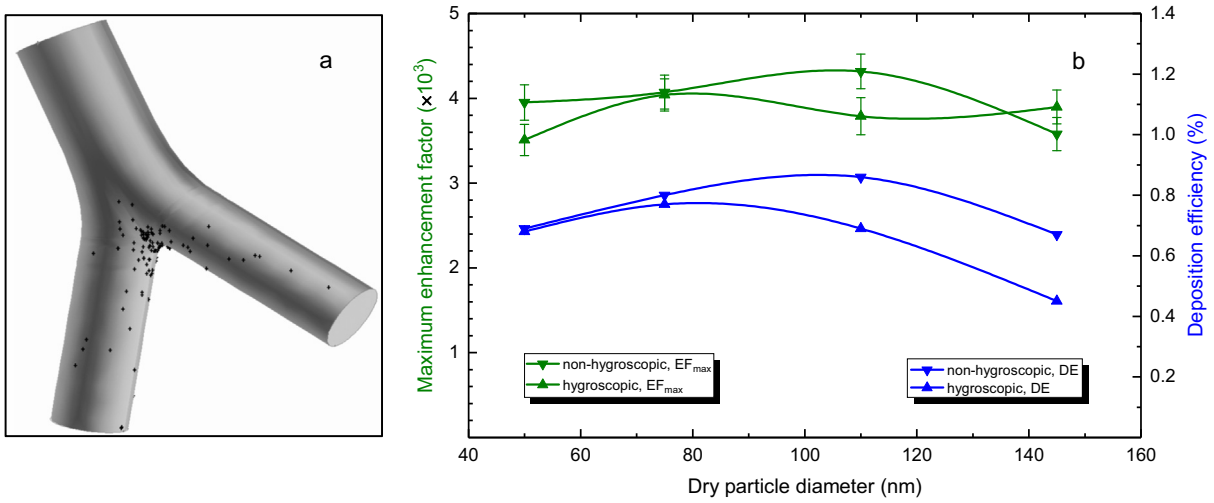

Fig. 4. Local deposition pattern of particles with a diameter of 110 nm in an airway bifurcation representing the 4th–5th airway generation considering their hygroscopic growth (a). Maximum enhancement factor (EF_{max}) and deposition efficiency (DE) values of particles with diameters of 50, 75, 110 and 145 nm in the same central airway bifurcation with and without considering the hygroscopic growth (b).

3.3. Local deposition in healthy subjects

The computed deposition pattern of hygroscopic monodisperse particles with a diameter of 110 nm in the selected central airway bifurcation is demonstrated in Fig. 4a. It confirms that the local deposition remained highly site specific with the highest deposition density in the vicinity of the bifurcation peak. There were areas which contained thousands times more particles than the average number of particles per unit surface area. The maximum values of the enhancement factors together with the deposition efficiency without and with considering the hygroscopic growth are shown in Fig. 4b. The mean value of the relative deposition efficiency decrease was approximately 15% (calculated by averaging the differences from Fig. 4b), which agrees with the results obtained by the Stochastic Lung Model for the lung (Fig. 2). The difference between the dry and hygroscopic particles in the deposition efficiency increased monotonically with particle size, which is also in line with the previous results and the ideas on urban-type aerosol. At the same time, no obvious tendency could be identified in the enhancement factors for the studied size range. The observed minor differences can be attributed to the stochastic nature of deposition by diffusion and the numerical error of the computational method (which was also marked in Fig. 4b).

3.4. Regional deposition in COPD patients

Our computations for COPD patients indicated that the deposition fractions of particles with a dry diameter of 50, 75, 110 and 145 nm decreased by 9.2%, 12.1%, 13.1% and 13.7% due to the hygroscopic growth in the ET region with respect to the dry particles. This implies that the tendencies observed for healthy subjects remained valid for them as well.

In the COPD-compromised lung, the effect of the hygroscopic growth on the depositions sensitively depended on the actual anatomical region (Fig. 5). Similarly to the healthy subjects, the hygroscopic growth of particles caused a decrease in the deposition fractions in the tracheobronchial region. The decrease was substantial (15–20%),

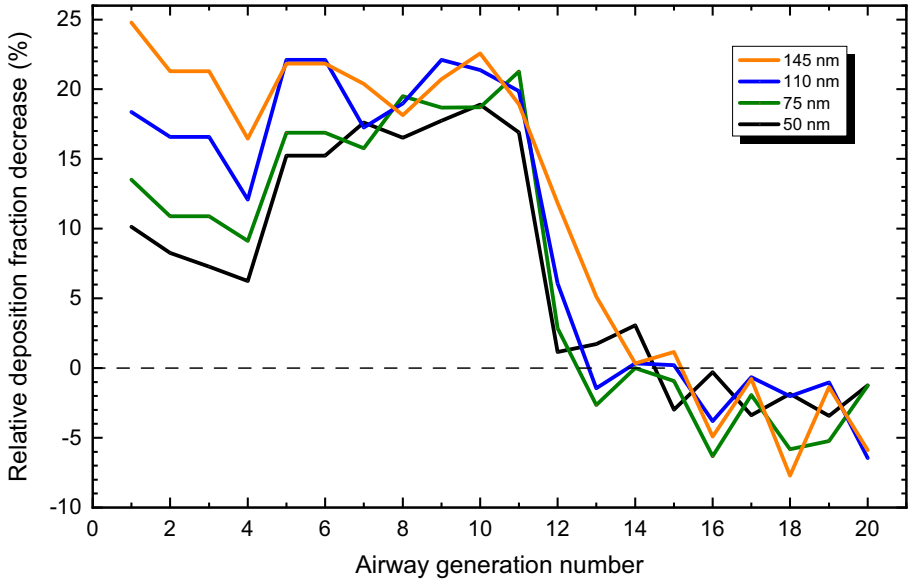

Fig. 5. Relative decrease of particle number deposition fractions in the airway generations of COPD patients due to hygroscopic growth for urban particles with different diameters.

which seemed somewhat lower than for the healthy airways. This can be explained by the special breathing patterns and airway geometry of the diseased population. In COPD patients, the bronchial and bronchiolar ducts are constricted (in our model by 25% in general) and the breathing flow rate in the bronchi is higher. The deposition is still diffusion driven, but diffusion becomes less pronounced. As a consequence, the decrease of the deposition fractions due to hygroscopic growth was lower in the conductive region of COPD patients than in the similar airway region of their healthy counterparts. Fig. 5 also demonstrates that the decrease of the deposition in the bronchi was generally higher for larger particles. This was driven mainly by the larger HGFs of larger particles (Table2).

In contrast to the results for healthy airways, the deposition of hygroscopic particles in the acinar region of the COPD patients appeared to be higher from airway generation 16 than for the dry particles. (Again, negative values actually represent deposition increase since it is the decrease that is shown.) This special deposition pattern was a result of altered acinar airway geometry. In COPD patients, the acinar ducts can be severely constricted (by 30–100% in our model) or even blocked. In these highly narrowed airways, the deposition by sedimentation does play a key role. Since the deposition by sedimentation increases by particle size, hygroscopic growth caused a moderate increase in the deposition fraction in the deep acinar airways. The extent of the increase depends on the severity of the disease. Furthermore, the comparison of the shapes of Figs. 3 and 5 clearly demonstrates that the airway disease can substantially modify the tendencies observed for healthy subjects.

4. Conclusions

Characterization of the airway deposition of inhaled urban-type aerosol in the human respiratory system is an important step in assessing their health effects. Some of these particles can extract water from the air at the high RH in the respiratory tract. We showed here that the hygroscopic particle diameter growth inside the airways modified the deposition patterns, especially those of UF aerosol. The particles were deposited with lower efficiency in the airways of healthy subjects after their hygroscopic growth. This is in contrast to the hygroscopic supermicrometer particles, for which the deposition fractions ordinarily increase after their growth. The actual extent of the decrease for the UF particles depended on the airway generation number, so it differed in various regions of the respiratory system. The relative decrease of particle number deposition fractions was 7–16% in the ET region, more substantial in the conductive airways (up to 25%) and less pronounced towards the terminal airways. At the local level, however, the hygroscopic growth did not influence the highly inhomogeneous nature of the deposition within a central bifurcation unit with some areas containing thousands times more particles than the average number of particles per unit surface area. In COPD patients, the hygroscopic growth affected the particle deposition differently. We observed a substantial relative decrease in the conductive airways, whereas the relative deposition increased in the acinar region.

On the one hand, the presence of the airway disease should be taken into account when assessing health consequences of inhaled ambient or workplace aerosols when elaborating protective measures for some sensitive population groups. On the other hand, the results also indicate some potentials for precision medical therapy or imaging diagnostics tailored to individuals by refining the dedicated drug delivery via hygroscopic adjustment of engineered nanoparticles.

Due to their size distribution, special chemical composition and mixing state, the hygroscopicity of urban-type particles was shown to be substantially and systematically smaller than for regional and remote locations (Salma et al., 2021). This also suggests that the differences observed in the present study could be even larger for non-urban locations.

CRediT authorship contribution statement

Árpád Farkas: lung deposition modelling, methodology, visualization, interpreting the results, writing. **Péter Füri**: lung deposition modelling, methodology, interpreting the results. **Wanda Thén**: data treatment, analysis, investigations, visualization. **Imre Salma**: conceptualization, data evaluation, supervision, writing.

Declaration of competing interest

The authors declare that they have no known competing financial interests or personal relationships that could have appeared to influence the work reported in this paper.

Acknowledgement

This research has been supported by the Hungarian Research, Development and Innovation Office (grant no. K132254).

References

Aaltonen, H.L., Jakobsson, J.K., Diaz, S., Zackrisson, S., Piitulainen, E., Londahl, J., Wollmer, P., 2018. Deposition of inhaled nanoparticles is reduced in subjects with COPD and correlates with the extent of emphysema: proof of concept for a novel diagnostic technique. Clin. Physiol. Funct. Imaging https://doi.org/10.1111/cpf.12517.

Apte, J.S., Marshall, J.D., Cohen, A.J., Brauer, M., 2015. Addressing global mortality from ambient PM2.5. Environ. Sci. Technol. 49, 8057–8066. https://doi.org/10.1021/acs.est.5b01236.

Asgharian, B., Price, O., Miller, F., Subramaniam, R., Cassee, F.R., Freijer, J., van Bree, L., Winter-Sorkina, R., 2009. Multiple-path Particle Dosimetry Model (MPPD v 2.11): A Model for Human and Rat Airway Particle Dosimetry. Applied Research Associates, Hamner Institutes for Health Sciences, National Institute for Public Health and the Environment and Ministry of Housing, Spatial Planning and the Environment, Raleigh, North Carolina, USA.

Balásházy, I., Alföldy, B., Molnár, A.J., Hofmann, W., Szőke, I., Kis, E., 2007. Aerosol drug delivery optimization by computational methods for the characterization of total and regional deposition of therapeutic aerosols in the respiratory system. Curr. Comp. Aided Drug Des. 3, 13–32. https://doi.org/10.2174/157340907780058727.

Balásházy, I., Horváth, A., Sárkány, Z., Farkas, Á., Hofmann, W., 2009. Simulation and minimisation of the airway deposition of airborne bacteria. Inhal. Toxicol. 21, 1021–1029. https://doi.org/10.1080/08958370902736646.

Bates, A.J., Doorly, D.J., Cetto, R., Calmet, H., Gambaruto, A.M., Tolley, N.S., Houzeaux, G., Schroter, R.C., 2015. Dynamics of airflow in a short inhalation. J. R. Soc. Interface 12, 20140880. https://doi.org/10.1098/rsif.2014.0880.

Braakhuis, H.M., Park, M.V., Gosens, I., De Jong, W.H., Cassee, F.R., 2014. Physicochemical characteristics of nanomaterials that affect pulmonary inflammation. Part. Fibre Toxicol. 11 (2014), 18. https://doi.org/10.1186/1743-8977-11-18.

Carvalho, T.C., Peters, J.I., Williams 3rd, R.O., 2011. Influence of particle size on regional lung deposition – what evidence is there? Int. J. Pharm. 406, 1–10. https://doi.org/10.1016/j.ijpharm.2010.12.040.

Choi, S., Yoon, S., Jeon, J., Zou, C., Choi, J., Tawhai, M.H., Hoffman, E.A., Delvadia, R., Babiskin, A., Walenga, R., Lin, C.L., 2019. 1D network simulations for evaluating regional flow and pressure distributions in healthy and asthmatic human lungs. J. Appl. Physiol. 127, 122–133.. https://doi:10.1152/jappl-physiol.00016.2019.

Cohen, A.J., Brauer, M., Burnett, R., Anderson, H.R., 2017. Estimates and 25-year trends of the global burden of disease attributable to ambient air pollution: an analysis of data from the global burden of diseases study 2015. Lancet 389, 1907–1918. https://doi.org/10.1016/S0140-6736(17)30505-6.

Devalia, J.L., Sapsford, R.J., Wells, C.W., Richman, P., Davies, R.J., 1990. Culture and comparison of human bronchial and nasal epithelial cells in vitro. Respir. Med. 84, 303–312. https://doi.org/10.1016/s0954-6111(08)80058-3.

Dua, S.K., Hopke, P.K., 1996. Hygroscopicity of indoor aerosols and its influence on the deposition of inhaled radon decay products. Environ. Int. 22, 941–947. https://doi.org/10.1016/S0160-4120(96)00206-1.

Enroth, J., Mikkilä, J., Németh, Z., Kulmala, M., Salma, I., 2018. Wintertime hygroscopicity and volatility of ambient urban aerosol particles. Atmos. Chem. Phys. 18, 4533–4548. https://doi.org/10.5194/acp-18-4533-2018.

Farkas, Á., Balásházy, I., 2008. Quantification of particle deposition in asymmetrical tracheobronchial model geometry. Comp. Biol Med. 35, 508–518. https://doi.org/10.1016/j.compbiomed.2008.01.014.

Farkas, Á., Lizal, F., Jedelsky, J., Elcner, J., Horváth, A., Jicha, M., 2019. Simulation of airway deposition of an aerosol drug in COPD patients. Pharmaceutics 11, 153. https://doi.org/10.3390/pharmaceutics11040153.

Farkas, Á., Lizal, F., Jedelsky, J., Elcner, J., Karas, J., Belka, M., Misik, O., Jicha, M., 2020. The role of combined use of experimental and computational methods in revealing the differences between the micron-size particle deposition patterns in healthy and asthmatic subjects. J. Aerosol Sci. 147, 105582. https://doi.org/10.1016/j.aerosci.2020.105582.

Fergusson, G.T., 2006. Why does the lung hyperinflate? Proc. Am. Thorac. Soc. 3, 176–179. https://doi.org/10.1513/pats.200508-094DO.

Ferron, G.A., 1977. The size of soluble aerosol particles as a function of humidity of the air. Application to the human respiratory tract. J. Aerosol Sci. 8, 251–267. https://doi.org/10.1016/0021-8502(77)90045-3.
Füri, P., Hofmann, W., Jókay, Á., Balásházy, I., Moustafa, M., Czitrovszky, B., Kudela, G., Farkas, Á., 2017. Comparison of airway deposition distributions of particles in healthy and diseased workers in an egyptian industrial site. Inhal. Toxicol. 29, 147–159. https://doi.org/10.1080/08958378.2017.1326990.
Gysel, M., McFiggans, G.B., Coe, H., 2009. Inversion of tandem differential mobility analyser (TDMA) measurements. J. Aerosol Sci. 40, 134–151. https://doi.org/10.1016/j.jaerosci.2008.07.013.
Haefeli-Bleuer, B., Weibel, E.R., 1988. Morphometry of the human pulmonary acinus. Anat. Records 220, 401–414. https://doi.org/10.1002/ar.1092200410.
Harrison, R.M., Jones, A.M., 2005. Multisite study of particulate number concentrations in urban air. Environ. Sci. Technol. 39, 6063–6070. https://doi.org/10.1021/es040541e.
Heal, M.R., Kumar, P., Harrison, R.M., 2012. Particles, air quality, policy and health. Chem. Soc. Rev. 41, 6606–6630. https://doi.org/10.1039/C2CS35076A.
HEI, 2013. Review panel on ultrafine particles: understanding the health effects of ambient ultrafine particles. HEI Perspectives 3. Health Effects Institute, Boston, MA.
Hofmann, W., 2011. Modelling inhaled particle deposition in the human lung - a review. J. Aerosol Sci. 42, 693–724. https://doi.org/10.1016/j.jaerosci.2011.05.007.
Hofmann, W., Koblinger, L., 1990. Monte Carlo modelling of aerosol deposition in human lungs. Part II: deposition fractions and their sensitivity to parameter variations. J. Aerosol Sci. 21, 675–688. https://doi.org/10.1016/0021-8502(90)90122-E.
Hofmann, W., Koblinger, L., 1992. Monte Carlo modelling of aerosol deposition in human lungs. Part III: comparison with experimental data. J. Aerosol Sci. 23, 51–63. https://doi.org/10.1016/0021-8502(92)90317-O.
Horváth, A., Balásházy, I., Farkas, Á., Sárkány, Z., Hofmann, W., Czitrovszky, A., Dobos, E., 2009. Quantification of airway deposition of intact and fragmented pollens. Int. J. Environ. Health Res. 21, 427–440. https://doi.org/10.1080/09603123.2011.574269.
ICRP (International Commission on Radiological Protection), 1994. Publication 66, Human respiratory tract model forradiological protection. Annals of the ICRP 24. Pergamon Press, Oxford, UK.
Ingelstedt, S., 1956. Studies on the conditioning of air in the respiratory tract. Acta Oto-Lar 131 (Supplement).
Jakobsson, J.K., Aaltonen, H.L., Nicklasson, H., Gudmundsson, A., Rissler, J., Wollmer, P., Löndahl, J., 2018. Altered deposition of inhaled nanoparticles in subjects with chronic obstructive pulmonary disease. BMC Pulm. Med. 18, 129. https://doi.org/10.1186/s12890-018-0697-2.
Keck, T., Leiacker, R., Heinrich, A., Kühnemann, S., Rettinger, G., 2000. Humidity and temperature profile in the nasal cavity. Rhinology 38, 161–171. https://doi.org/10.1097/00005537-200004000-00021.
Koblinger, L., Hofmann, W., 1990. Monte Carlo modeling of aerosol deposition in human lungs. Part I: simulation of particle transport in a stochastic lung structure. J. Aerosol Sci. 21, 661–674. https://doi.org/10.1016/0021-8502(90)90121-D.
Kreyling, W.G., Semmler, M., Erbe, F., Mayer, P., Takenaka, S., Schulz, H., Oberdörster, G., Ziesenis, A., 2002. Translocation of ultrafine insoluble iridium particles from lung epithelium to extrapulmonary organs is size dependent but very low. J. Toxicol. Environ. Health A 65, 1513–1530. https://doi.org/10.1080/00984100290071649.
Kreyling, W.G., Semmler-Behnke, M., Möller, W., 2006. Ultrafine particle-lung interactions: does size matter? J. Aerosol Med. 19, 74–83. https://doi.org/10.1089/jam.2006.19.74.
Kristensson, A., Rissler, J., Löndahl, J., Johansson, C., Swietlicki, E., 2013. Size-resolved respiratory tract deposition of sub-micrometer aerosol particles in a residential area with wintertime wood combustion. Aerosol Air Qual. Res. 13, 24–35. https://doi.org/10.4209/aaqr.2012.07.0194.
Lelieveld, J., Evans, J.S., Fnais, M., Giannadaki, D., Pozzer, A., 2015. The contribution of outdoor air pollution sources to premature mortality on a global scale. Nature 525, 367–371. https://doi.org/10.1038/nature15371.
Liu, P.F., Zhao, C.S., Göbel, T., Hallbauer, E., Nowak, A., Ran, L., Xu, W.Y., Deng, Z.Z., Ma, N., Mildenberger, K., Henning, S., Stratmann, F., Wiedensohler, A., 2011. Hygroscopic properties of aerosol particles at high relative humidity and their diurnal variations in the North China plain. Atmos. Chem. Phys. 11, 3479–3494. https://doi.org/10.5194/acp-11-3479-2011.
Löndahl, J., Massling, A., Pagels, J., Swietlicki, E., Vaclavik, E., Loft, S., 2007. Size-resolved respiratory-tract deposition of fine and ultrafine hydrophobic and hygroscopic aerosol particles during rest and exercise. Inhal. Toxicol. 19, 109–116. https://doi.org/10.1080/08958370601051677.
Löndahl, J., Möller, W., Pagels, J.H., Kreyling, W.G., Swietlicki, E., Schmid, O., 2014. Measurement techniques for respiratory tract deposition of airborne nanoparticles: a critical review. J Aerosol. Med. Pulm. Drug Deliv. 27, 229–254.
Massling, A., Niedermeier, N., Hennig, T., Fors, E.O., Swietlicki, E., Ehn, M., Hämeri, K., Villani, P., Laj, P., Good, N., McFiggans, G., Wiedensohler, A., 2011. Results and recommendations from an intercomparison of six hygroscopicity-TDMA systems. Atmos. Meas. Tech. 4, 485–497. https://doi.org/10.5194/amt-4-485-2011.
Mikkonen, S., Németh, Z., Varga, V., Weidinger, T., Leinonen, V., Yli-Juuti, T., Salma, I., 2020. Decennial time trends and diurnal patterns of particle number concentrations in a central european city between 2008 and 2018. Atmos. Chem. Phys. 20, 12247–12263. https://doi.org/10.5194/acp-20-12247-2020.
Morawska, L., Ristovski, Z., Jayaratne, E.R., Keogh, D.U., Ling, X., 2008. Ambient nano and ultrafine particles from motor vehicle emissions: characteristics, ambient processing and implications on human exposure. Atmos. Environ. 42, 8113–8138. https://doi.org/10.1016/j.atmosenv.2008.07.050.
O'Donnell, D.E., Revill, S.M., Webb, K.A., 2001. Dynamic hyperinflation and exercise intolerance in chronic obstructive pulmonary disease. Am. J. Respir. Crit. Care Med. 164, 770–777. https://doi.org/10.1164/ajrccm.164.5.2012122.
Oberdörster, G., Oberdörster, E., Oberdörster, J., 2005. Nanotoxicology: an emerging discipline evolving from studies of ultrafine particle. Environ. Health Perspect. 113, 823–839. https://doi.org/10.1289/ehp.7339.
Papandrinopoulou, D., Tzouda, V., Tsoukalas, G., 2012. Lung compliance and chronic obstructive pulmonary disease. Pulm. Med., 542769 https://doi.org/10.1155/2012/542769 6 ps.
Perwitzschky, R., 1928. Die temperature and feuchtigkeitsverhaltnisse der atemluft in den luftwegen. J. Mitt. Arch. Ohren Nasen Kehlkopf 117, 1.
Raabe, O.G., Yeh, H.-C., Schum, G.M., Phalen, R.F., 1976. Tracheo-bronchial geometry: human, dog, rat, hamster – a compilation of selected data from the project respiratory tract deposition models. Report LF-53. Lovelace Foundation, Albuquerque, NM.
Rajaraman, P.K., Choi, J., Hoffman, E.A., O'Shaughnessy, P.T., Choi, S., Delvadia, R., Babiskin, A., Walenga, R., Lin, C.-L., 2020. Transport and deposition of hygroscopic particles in asthmatic subjects with and without airway narrowing. J. Aerosol Sci. 146 (105581), 1–15. https://doi.org/10.1016/j.jaerosci.2020.105581.
Riediker, M., Zink, D., Kreyling, W., Oberdörster, G., Elder, A., Graham, U., Lynch, I., Duschl, A., Ichihara, G., Ichihara, S., Kobayashi, T., Hisanaga, N., Umezawa, M., Cheng, T.-J., Handy, R., Gulumian, M., Tinkle, S., Cassee, F., 2019. Particle toxicology and health - where are we? Part. Fibre Toxicol. 16, 19. https://doi.org/10.1186/s12989-019-0302-8.
Rissler, J., Vestin, A., Swietlicki, E., Fisch, G., Zhou, J., Artaxo, P., Andreae, M.O., 2006. Size distribution and hygroscopic properties of aerosol particles from dry-season biomass burning in Amazonia. Atmos. Chem. Phys. 6, 471–491. https://doi.org/10.5194/acp-6-471-2006.
Salma, I., Balásházy, I., Winkler-Heil, R., Hofmann, W., Záray, Gy, 2002. Effect of particle mass size distribution on the deposition of aerosols in the human respiratory system. J. Aerosol. Sci. 33, 119–132. https://doi.org/10.1016/S0021-8502(01)00154-9.
Salma, I., Füri, P., Németh, Z., Balásházy, I., Hofmann, W., Farkas, Á., 2015. Lung burden and deposition distribution of inhaled atmospheric urban ultrafine particles as the first step in their health risk assessment. Atmos. Environ. 104, 39–49. https://doi.org/10.1016/j.atmosenv.2014.12.060.
Salma, I., Németh, Z., Weidinger, T., Kovács, B., Kristóf, G., 2016. Measurement, growth types and shrinkage of newly formed aerosol particles at an urban research platform. Atmos. Chem. Phys. 16, 7837–7851. https://doi.org/10.5194/acp-16-7837-2016.
Salma, I., Vasanits-Zsigrai, A., Machon, A., Varga, T., Major, I., Gergely, V., Molnár, M., 2020. Fossil fuel combustion, biomass burning and biogenic sources of fine carbonaceous aerosol in the Carpathian Basin. Atmos. Chem. Phys. 20, 4295–4312. https://doi.org/10.5194/acp-20-4295-2020.
Salma et al., n.d. I. Salma W. Thén M. Vörösmarty A. Z. Gyöngyösi : Cloud activation properties of aerosol particles in a continental central European urban environment, Atmos. Chem. Phys., 21, 11289–11302, doi:10.5194/acp-21-11289-2021.
Sturm, R., 2016. Local lung deposition of ultrafine particles in healthy adults: experimental results and theoretical predictions. Ann. Transl. Med. 4, 420. https://doi.org/10.21037/atm.2016.11.13.
Swietlicki, E., Hansson, H.C., Hämeri, K., Svenningsson, B., Massling, A., McFiggans, G., McMurry, P.H., Petäjä, T., Tunved, P., Gysel, M., Topping, D., Weingartner, E., Baltensperger, U., Rissler, J., Wiedensohler, A., Kulmala, M., 2008. Hygroscopic properties of submicrometer atmospheric aerosol particles measured with H-TDMA instruments in various environments – a review. Tellus B 60, 432–469. https://doi.org/10.1111/j.1600-0889.2008.00350.x.
Valavanidis, A., Fiotakis, K., Vlachogianni, T., 2008. Airborne particulate matter and human health: toxicological assessment and importance of size and composition of particles for oxidative damage and carcinogenic mechanisms. J. Environ. Sci. Health C 26, 339–362. https://doi.org/10.1080/10590500802494538.
Vu, T.V., Delgado-Saborit, J.M., Harrison, R.M., 2015. A review of hygroscopic growth factors of submicron aerosols from different sources and its implication for calculation of lung deposition efficiency of ambient aerosols. Air Qual. Atmos. Health 8, 429–440. https://doi.org/10.1007/s11869-015-0365-0.
Vu, T.V., Ondráček, J., Ždímal, V., Schwarz, J.S., Delgado-Saborit, J.M., Harrison, R.M., 2017. Physical properties and lung deposition of particles emitted from five major indoor sources. Air Qual. Atmos. Health 10, 1–14. https://doi.org/10.1007/s11869-016-0424-1.
Vu, T.V., Shi, Z., Harrison, R.M., 2021. Estimation of hygroscopic growth properties of source-related sub-micrometre particle types in a mixed urban aerosol. Clim. Atmos. Sci. 4, 21. https://doi.org/10.1038/s41612-021-00175-w.
Winkler-Heil, R., Ferron, G., Hofmann, W., 2014. Calculation of hygroscopic particle deposition in the human lung. Inhal. Toxicol. 26, 193–206. https://doi.org/10.3109/08958378.2013.876468.